Effect of the vacancy on the electrical transport properties of boron nitride nanosheets

Neda Dehghan, Mohammad Reza Niazian *, Mojtaba Yaghobi , Mohammad Ali Ramzanpour

Department of Physics, Ayatollah Amoli Branch, Islamic Azad University, Amol, Iran.

*Corresponding author: m.reza.niazian@gmail.com

Abstract:

Vacancies occur naturally in all crystalline materials. A vacancy is a point defect in a crystal in which an atom is removed at one of the lattice sites. The defect could be imported during the synthesis of the material or be added by defect engineering. In this paper by employing the density functional theory as well as the non-equilibrium Green's function approach, the structure and electronic properties of the perfect and defected BN nanosheet would be obtained and compared.

In addition to the influence of the vacancy defect position, the effect of removed atom type is also studied. For this purpose, the defect is considered at the center, left, and right hand sides of the nanosheet. It is seen that the electric current changes by changing the position of the vacancy defect and the type of removed atoms. This can be related to the electronic structures of BN nanosheets. In addition, the transmission and conductance of the defected BN nanosheets continuously change by changing the bias voltage.

The obtained results can benefit the design and implementation of BN nanosheets in nanoelectronic systems and devices.

Keywords: Point defect; BN nanosheets device; Slater–Koster tight-binding model; DFTB; Atomistix ToolKit; Electrical transport

1. Introduction

In recent years, molecular devices have been suggested as applicable components to be used in the future electronic circuits. To form such devices, one molecule or a group of molecules are considered in a layer arrangement which is connected to two or more electrodes. It has been shown that the transport characteristics of such molecular devices are affected by different factors including their electronic structures as well as physical and chemical properties of their constitutive molecules. In the structure of the molecular devices, molecules are considered as quantum dots. The discrete energy levels of these quantum dots are at least one order of magnitude smaller than the semiconductor quantum dots [1–3]. As a weak contact is created between the molecules and the electrodes, caused by the potential barriers, electronic isolation would be occur between the metallic electrodes and molecular quantum dots. Furthermore, if the molecular quantum dots are utilized for the conduction purposes, they could be thermally activated and vibrated at the finite temperatures. This behavior is not seen in the semiconductor quantum dots. Based on the interactions between the electrons and phonons, by Walczak and Zhou developed the Green's function approach to study the transport of the electron in the DNA molecules [4,5].

If the electrons are passed through some energetically accessible molecular states (i.e. conduction channels), the energy could be exchanged between the electrons and nuclear degrees of freedom. Hence, an inelastic component would be appeared in the current [6].

Recently, different approaches used for controlling this process have been applied. The molecular electronics is a developing research area whose purpose is to improve the efficiency of these devices.

Caused by the attractive chemical and physical properties of the fullerene, a spherical allotrope of carbon, several research groups have investigated the properties of fullerene-like structures which are made from other atoms, including the members of the groups III, IV and V of the periodic table [7]. Furthermore, some applications have been found for these fullerene-like structures. Similarly, 2D graphene-like
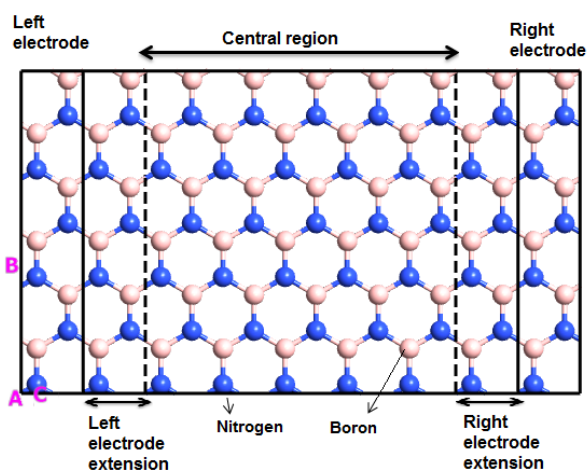
Figure 1. Configuration of the optimized BN Nanosheets device without the vacancy defect.

nanostructures have also been considered for investigation on their physical and chemical properties.

As a sample, boron nitride (BN) nanosheets, also called "white graphene", may be a good candidate to alternate graphene in some applications. Having desirable physical properties, including mechanical properties, impermeability, and thermal conductivity boron nitride (BN) nanosheets would not cause galvanic corrosion. Moreover, due to wider bandgap than graphene, more transparency to visible light is observed in the BN nanosheets than the graphene. Besides, BN nanosheets are more chemically and thermally stable than the graphene [8].

It has been shown that the BN nanosheets possess thermal and chemical stabilities larger than graphene. Moreover, a significant charge transfer is observed from B to N atoms. Hence, B-N bonds which are partially ionic sp^2-hybridized leads to notably different optics and electronics properties in BN nanosheets from graphene. For example, the color of BN is white with a large bandgap of 5.5 eV. While the color of graphene is black and it is conductive [9]. Due to these unusual structures and characteristics, BN nanosheets have found diverse functionalities. They are intrinsic insulators which make them as a valuable choice for dielectric applications for example to be used as a dielectric gate layer and ultraviolet luminescent agent [10].

One of the most important properties of the BN nanosheets is that they are electrically insulating and do not increase the galvanic corrosion of the underlying metal. The chemical vapour deposition (CVD) approach can be used to synthesize the BN nanosheets with relatively large sizes [11]. In many practical applications, the anti-oxidation protection of the metals at low temperatures for a considerably long time is of great importance. Similar to the graphene, BN nanosheets can be employed as an anti-corrosion coating on the metal substrates or some arbitrary other substrates. It has been reported that the copper surface can be protected from oxidation at 500 °C for 0.5 h by adding a BN nanosheet layer with the thickness of 0.5 nm [12]. In recent years, the construction of electronic structures of boron nitride through point defect design has become widespread. The

point defects during synthesis can alter the nanostructured properties of BN [13].

The investigation of the nanostructures having different types of defeats is of great importance. The considered defects in the literature are as vacancy, substitution, and interstitial defects.

In this paper, the transport properties of perfect and defective BN nanosheets are investigated. For this purpose, the single vacancy defect is considered at different positions on the structure of the nanosheet.

Since boron atom is deficient in electrons and nitrogen atom is rich of electrons, the properties of the BN nanosheets in the absence of boron and nitrogen atoms would be investigated, separately [14].

The transport, conductance and electronic properties of the BN nanosheets with and without single vacancy defect are evaluated. For this purpose, the density functional theory (DFT) is used.

2. Computational model

Here, the BN nanosheet with a single-vacancy defect is modeled.

The configurations of the optimized pure and defected BN nanosheet devices are given in Figs. 1, 2 and 3, respectively. As it can be seen in these figures, the position of the defect and the removed atom type are considered as the variables here.

As it can be seen in this figure, the vacancy defect is considered at different positions.

The first principle calculations are performed to optimize the geometry of the considered structures and calculate the electronic properties. For this purpose, the DFT is used along with the technique of non-equilibrium Green's function (NEGF). Semi-Empirical (SE) calculator can be used to model the electronic characteristics of molecules, crystals and devices. For this purpose, self-consistent and non-self-consistent tight-binding models can be employed. Here, tight-binding models are implemented based on Slater–Koster model [15].

In Slater–Koster tight-binding model, the density functional based tight binding (DFTB) formalism is closely followed which has been described in. In this model, a numerical function is used to express the distance-dependence of the matrix elements. In the DFTB approach, a second-order expansion of Kohn-Sham expression of the total energy with respect to the fluctuations of the charge density is used [16, 17]. The zeroth order method is considered as common standard non-self-consistent (TB) plan. While, in the second order approach, a transparent and parameter-free expression is derived for the elements of the generalized Hamiltonian matrix.

A device of the BN nanosheet is considered here and an electrode with the length of 2.46 Å is located at its left and right sides. Furthermore, the unit cell chiral vector C is selected as $n = 3$, $m = 3$ which is repeated along the $A = 1$, $B = 1$ and $C = 7$ axes after optimizing the device.

The Atomistix ToolKit (ATK) is used for all of the calculations. To depict the atom cores, Troullier–Martins normconserving pseudopotentials is employed which is
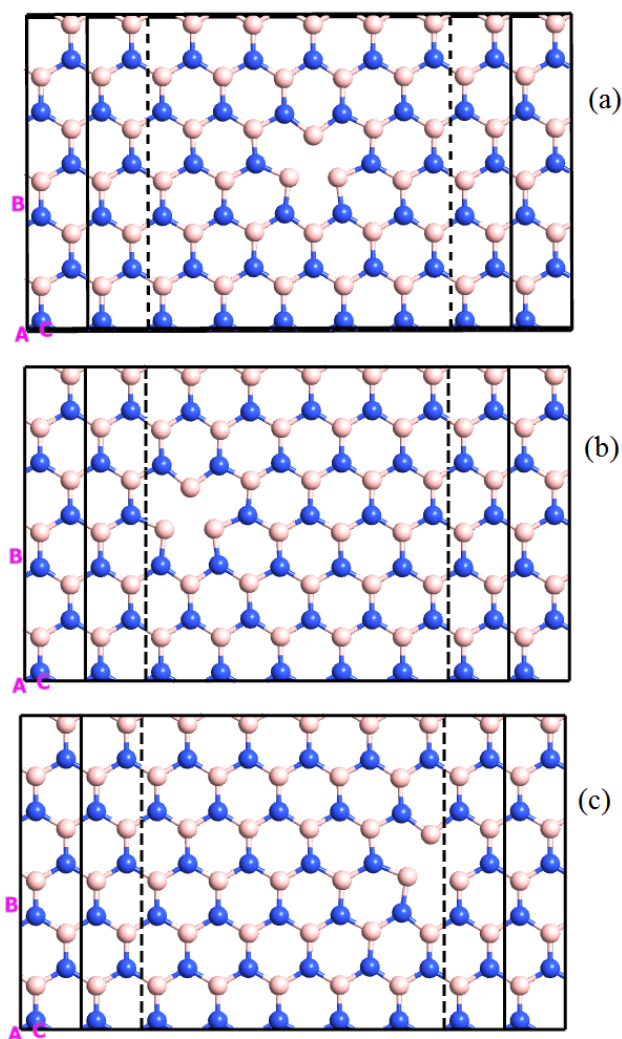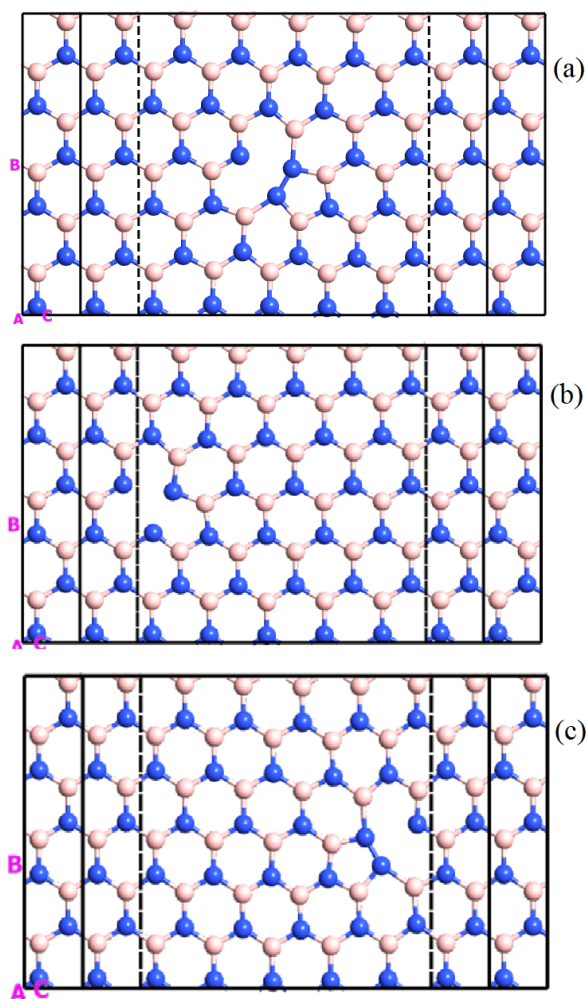
Figure 2. Configuration of the optimized BN Nanosheets device with a single vacancy (nitrogen removed). Vacancy defect is at (a) center, (b) left, and (c) right hand-side of the nanosheets.

Figure 3. Configuration of the optimized BN Nanosheets device with a single vacancy (boron removed). Vacancy defect is at (a) center, (b) left, and (c) right hand-side of the nanosheets.

also represent the linear combinations of atomic orbitals which can help to expand the valence states of electrons. The k-point is selected as (1 ,1 ,150) in the Brillouin zone and the electrode temperature is set as $T = 300$ K. Furthermore, the cutoff energy for the grid integration is considered as 150 Rydberg which is mainly used to control the size of the real space in the partitioning of the integral network and solving Poisson's equation [18, 19]. Quasi Newton approach is utilized for complete optimizing the atomic structures, including the atomic positions as well as the lattice parameters. Besides, the boundary conditions are considered as periodic. For all of the simulations, initially the geometry is optimized until all of the residual forces are smaller than 0.02 eV/Å.

3. Results and discussions

According to Figs. 1, 2 and 3, pure and defected BN nanosheet devices are investigated here. The position of the

defect and the type of the removed atom are variables.

To calculate the transport property of the BN nanosheets, the DFT is used in combination with Keldysh non-equilibrium Green's functions (NEGF) method. The calculations are performed by the Atomistix ToolKit (ATK) package [20–22]. Besides, using the local density approximation is implemented with the Slater–Koster model. As it was previously mentioned, the energy cutoff is used as 150 Rydberg to for the grid integration of the charge density. The k-point sampling is chosen as $1 \times 1 \times 150$ for calculation the transport properties and total energy. The numerical tolerance of 1×10^{-5} eV was used to control the NEGF-DFT self-consistency.

Figures 4 show the electronic band structure and total density of states (DOS) corresponding to the boron nitride nanosheet. In fact, DOS expresses the number of Eigen-stats of energy per unit of energy range and depends on the dispersion relation.

The results show that the boron nitride nanosheet has semi-conductor properties with a wide band gap of about 4.95
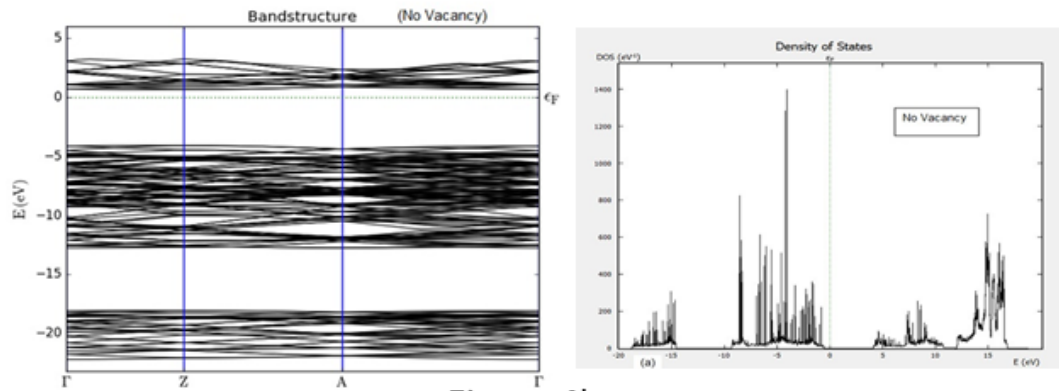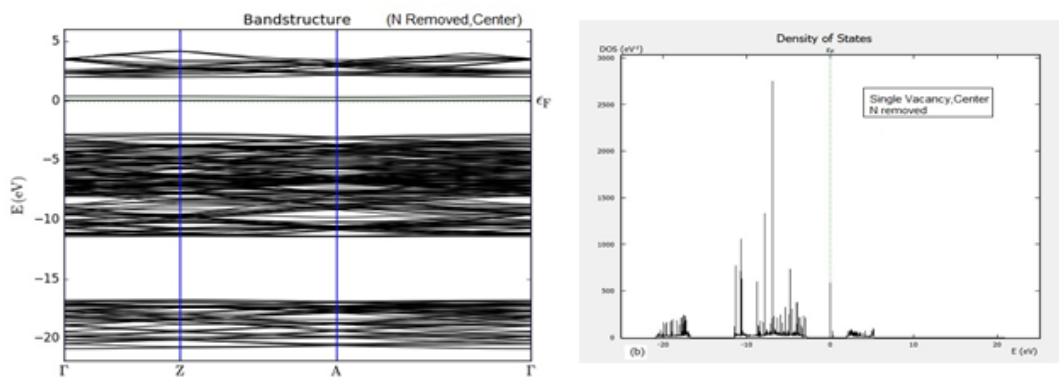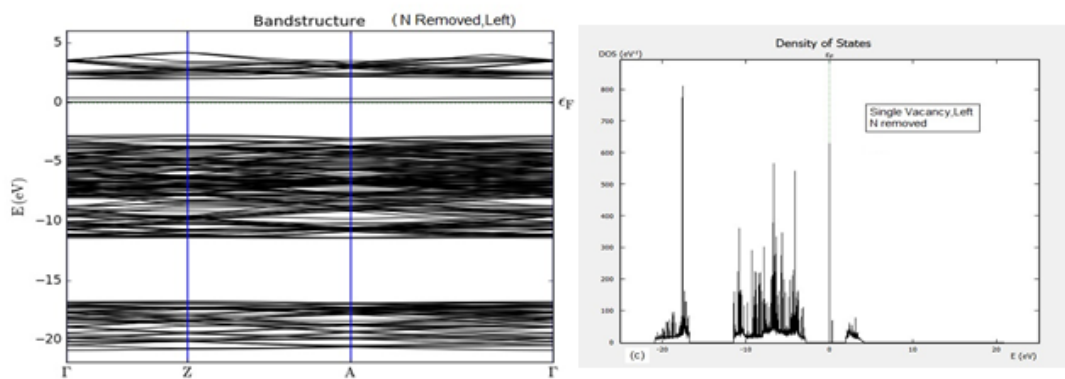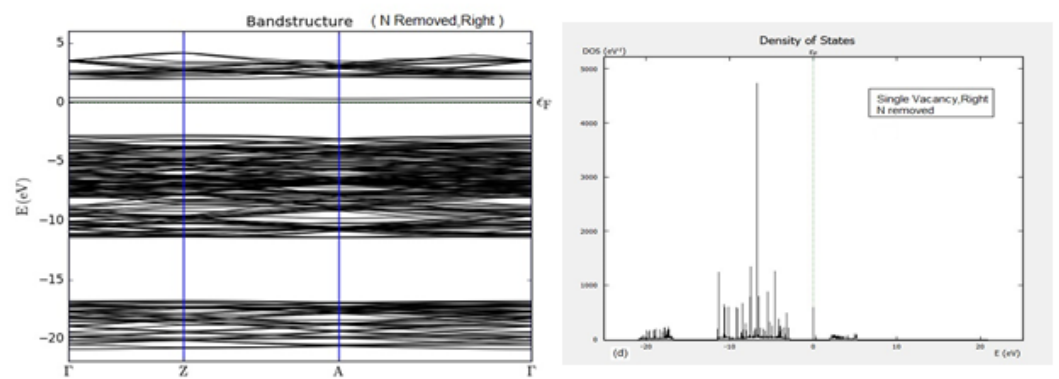
Figure 4a

Figure 4b

Figure 4c

Figure 4d

Figure 4e
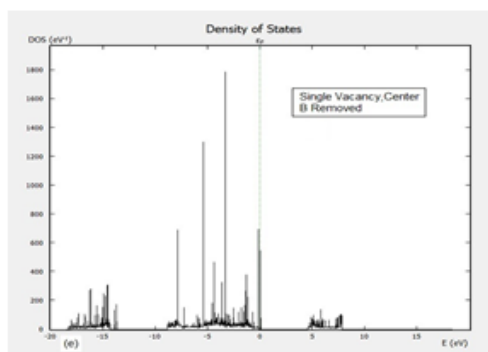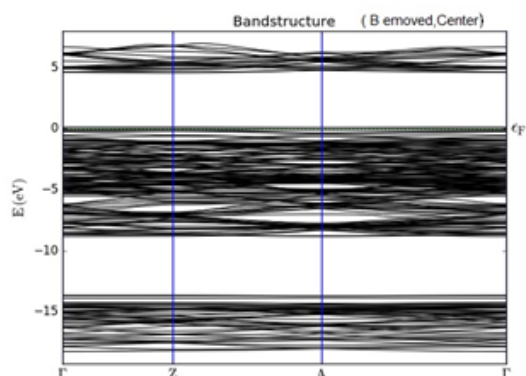
Figure 4f
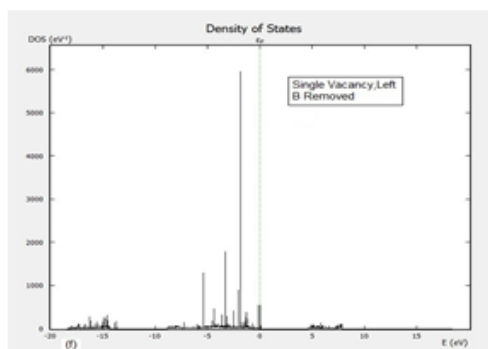
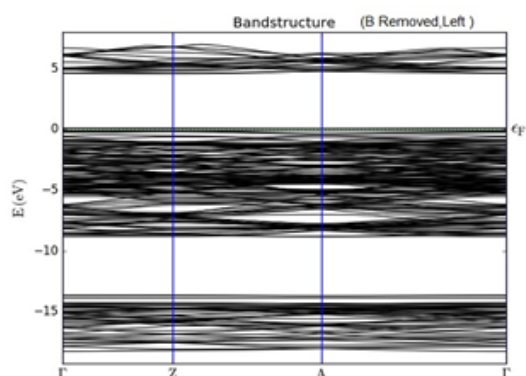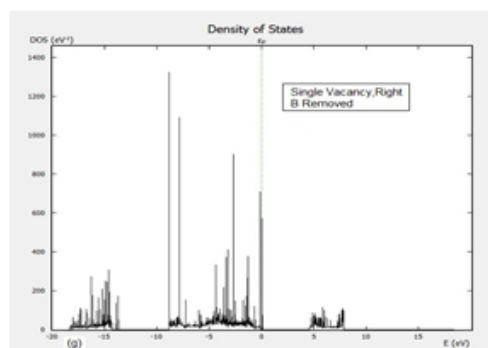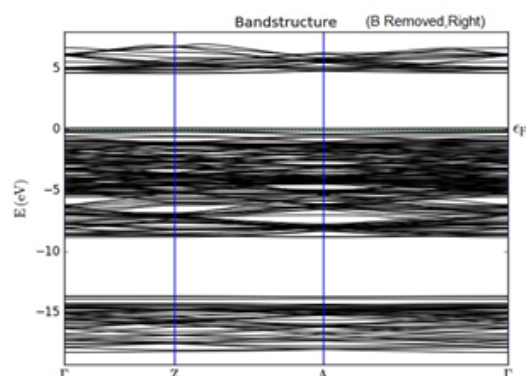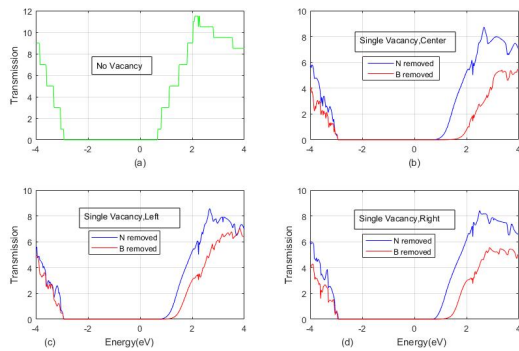## Figure 4g

Figure 4. The band structures and density of state (DOS) of the BN nanosheets in (a) Without the vacancy, N removed at (b) center, (c) left, (d) right and B removed at (e) center , (f) left, (g) right, respectively.

eV, which is above the valence band and below the conduction band located at the same point, and it shows that the h-BN nanosheet belongs to the direct band gap family. Also, in Figs. 4, the DOS of pure and defective BN nanosheets are shown as a function of E (eV), respectively. We have plotted the density of states of the defective BN nanosheets compared to the pure ones. The results show that the DOS with the defective and pure is very different. The defectives clearly change the DOS of BN nanosheets. Figures 4(b) to 4(g) compared to Figure 4(a) show that the peak height of the N removed in center of BN nanosheets increases greatly and the electron conduction increases because the availability of the state around Fermi energy increases.

Figs. 5 show the zero-bias transmission spectra of BN nanosheets versus energy for the nanosheets without and with vacancy defect. The results are given for the nanosheets in which the nitrogen and boron atoms are removed from different positions.

The steplike characteristics of spectra are related to the available conductance channels due to energy bands. When a defect occurs, the steplike behavior is gradually washed away, which is the results of the structural rupture and the plastic deformation of atomic configuration under defect. It can also be seen that the amplitudes of the transmission
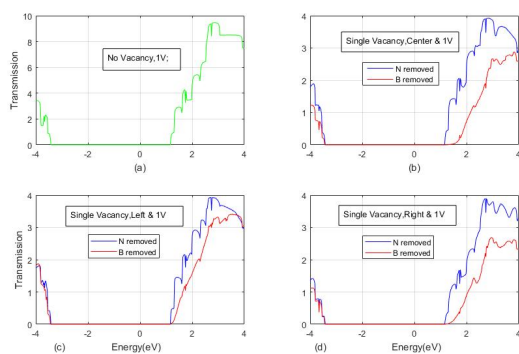
Figure 5. Transmission spectra of the defected BN nanosheets in which the nitrogen and boron atoms removed under zero-bias voltage (a) Without the vacancy, Vacancy defect at (b) center, (c) left, and (d) right hand-side of the nanosheets. The Fermi level is set to 0 eV.

Figure 7. Transmission spectra of the pure and defective BN nanosheet (nitrogen and boron removed) versus energy at 3 V voltages (a) Without the vacancy, Vacancy defect at (b) center, (c) left, and (d) right hand-side of the nanosheets.

spectrum are decreased for all vacancy defects with the removed nitrogen and boron atoms at different locations. The transmission decay can be attributed to the scattering barrier set by the local defect [23].
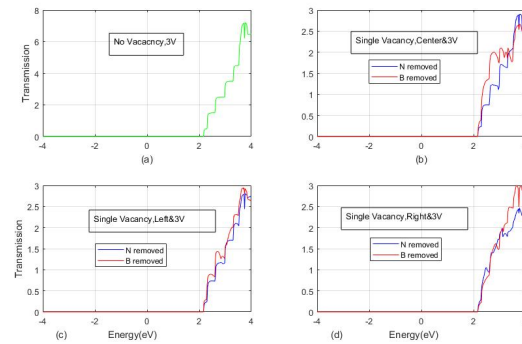
It can be seen that transmission peak threshold increase by increasing the voltage. Figs. 6 to 8 show the transmission spectra of the defective BN nanosheets in which the nitrogen and boron atoms has been removed, respectively. Here, the bias voltage is selected as 1, 3 and 5 V.

According to Figs. 6 to 8, it is clear that there are several similar transmission peaks in the same energy. Besides, the voltage range indicates that the transmission resonances depend on the defect. The step-like behavior of the calculated spectra is associated to the conductance channels caused by the energy bands. It can also be said that the undeformed BN nanosheet is a uniform system in which no considerable charge transfer is observed.

The step-like appearance of the transmission spectrum is also seen at higher voltages. However, at sufficiently large voltages, the step-like behavior would be gradually disappeared. Moreover, it is observed that the amplitudes of transmission spectra of the considered structures are de-
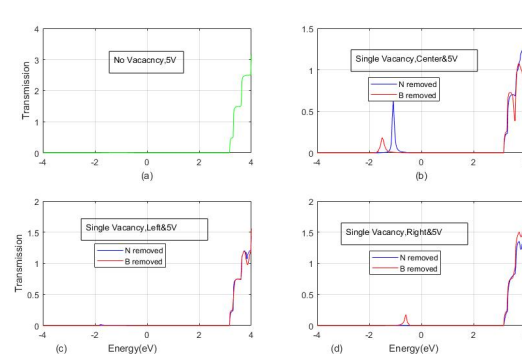
creased by increasing the voltage.

To further investigate the effect of position defect and atom type removed on the electrical transport of BN nanosheets, the I–V properties of each of the models are calculated and depicted in Figs. 9 and 10. The bias voltage is increased with the steps of 0.1 V. Besides, the converged density matrix of each state would be used as the initial guess of the next step. Landauer–Buttiker formula is used to obtain the current through BN nanosheet:

$$I(V) = \frac{2e}{h} \int_{\mu_L}^{\mu_R} T(E.V)[f(E,\mu_L) - f(E,\mu_R)]dE \quad (1)$$

In the above equation, e, h and V are the charge of the electron, Planck's constant, and the applied bias, receptively. Besides, $f(E,\mu)$ is the distribution of the Fermi–Dirac and μ_L and μ_R are the chemical potentials associated with the left and right electrodes, respectively. The integration between the lower and higher limits of μ_L and μ_R, respectively, is named as the bias window [24, 25].

According to Figures 9 and 10, no current is passed at low voltages for the defective BN nanosheets with both types of the removed atom.

By increasing the applied bias voltage, the current in the

Figure 6. Transmission spectra of the pure and defective BN nanosheet (nitrogen and boron removed) versus energy at 1 V voltages (a) Without the vacancy, Vacancy defect at (b) center, (c) left, and (d) right hand-side of the nanosheets.

Figure 8. Transmission spectra of the pure and defective BN nanosheet (nitrogen and boron removed) versus energy at 5 V voltages (a) Without the vacancy, Vacancy defect at (b) center, (c) left, and (d) right hand-side of the nanosheets.
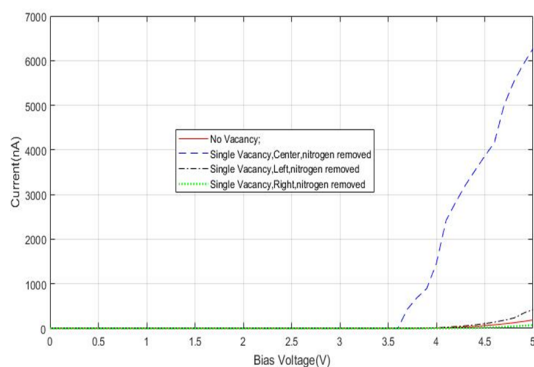
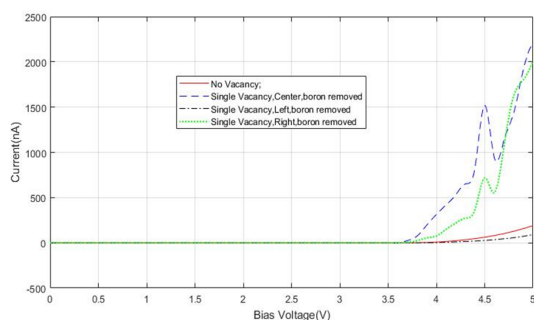**Figure 9.** I–V Characteristics of the pure and defective BN nanosheets (nitrogen removed).

Figure 11. Comparison of new the peak of transport the bias window for both of the single-vacancy defected BN nanosheets with removed nitrogen and boron from the center of the nanosheet versus energy at different voltages (a) 3.8 V, (b) 4 V, (c) 4.6 V and (d) 5 V.

I–V curves slowly increases up to a certain voltage and then a significant increase is seen in the current. This can be associated with the semiconductor characteristics of the BN nanosheets. The same behavior has also been observed for other semiconducting materials. In the geometrical configuration of the BN nanosheet with the electrodes, the Fermi level of the left electrode would be shifted with respect to the right electrode by applying a bias voltage [26–29]. If the energy of the top of the left electrode valence band matches with the bottom of the right electrode conduction band, the current would start to flow. In this situation, the bias voltage is approximately equal to the zero-bias band gap of system. However, for the finite bias voltage, the transport properties and electronic structures of the BN nanosheet is affected by the bias which results in a so-called effective band gap.
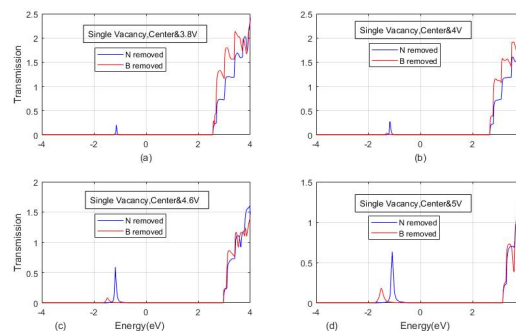
For a better understanding of the transport in the center of the nanosheet, in Figs. 11 the transmission spectra are drawn from the start of the peak in the bias window for both types of the removed atoms.

Comparison of Figures 11 shows that for both of the single-vacancy defected BN nanosheets with nitrogen and boron atoms removed from the center of the nanosheet, new the peak of transport the bias window begins to increase.

On the other hand, the comparison of these two figures shows that the peak height of the transport of the BN nanosheet with nitrogen removed atom is greater than that of BN nanosheet with boron removed atom. As a result, the current in the nitrogen removed BN nanosheet would

be larger than the nitrogen removed BN nanosheet which corresponds perfectly to Figs. 9 and 10 (blue dashed lines). Characteristics of spectra are related to the available conductance channels due to energy bands.

According to the curves, for the defected BN nanosheet in which a nitrogen atom has been removed from the center of the nanosheet, no current is observed until the bias voltage of 3.6 V. However, this value is 4.3 V for the perfect BN nanosheet and defected BN nanosheet in which a nitrogen atom has been removed from the left and right sides of the nanosheet.

Besides, for the defected BN nanosheet in which a boron atom has been removed from the center of the nanosheet current threshold is 3.7 V. This parameter is 3.8 V for the perfect 3.8 V BN nanosheet and defected nanosheets with the removed boron atom from the left and right hand side of the nanosheet.

We also investigate the electric current curve with the same position defect but different removed atoms. Furthermore, the electric current curve of the BN nanosheet with the different removed atom types from the same position is also represented here in Figs. 12.

According to this figure, the current passing through defected BN nanosheets with the nitrogen and boron removed atoms are different in left local. For example, at the bias voltage of 5 V, the current passing through the BN nanosheets with the nitrogen and boron atoms removed from the left side of the nanosheet are about 4.22×10^2 nA, and 9.13×10^1 nA, respectively. In other words, the electrical current of the BN nanosheet with the N atom removed is 4.62 times larger than that of the BN nanosheet with the B atom removed.

Furthermore, the electric currents are obtained as about 6.27×10^3 nA , and 2.2×10^3 nA, respectively for the nitrogen and boron atoms removed from the center position. The electric current for the BN nanosheet with nitrogen removed atom is 2.85 times the electric current for the BN nanosheet with boron removed atom. Moreover, currents are obtained as about 75.4 nA, and 2.01×10^3 nA, respectively for nitrogen and boron atom removed from the right position of the nanosheet. In this case, the electric current for the BN nanosheet with boron removed atom is 26.65 times the elec-
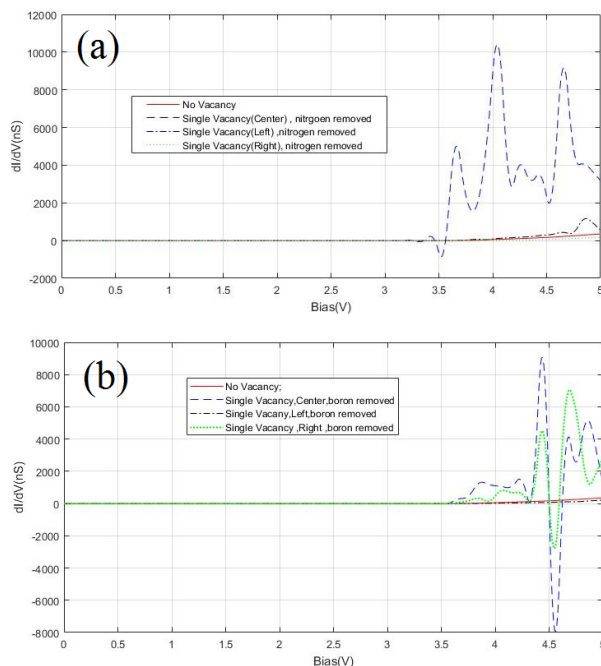

Figure 10. I–V Characteristics of the pure and defective BN nanosheets (boron removed).
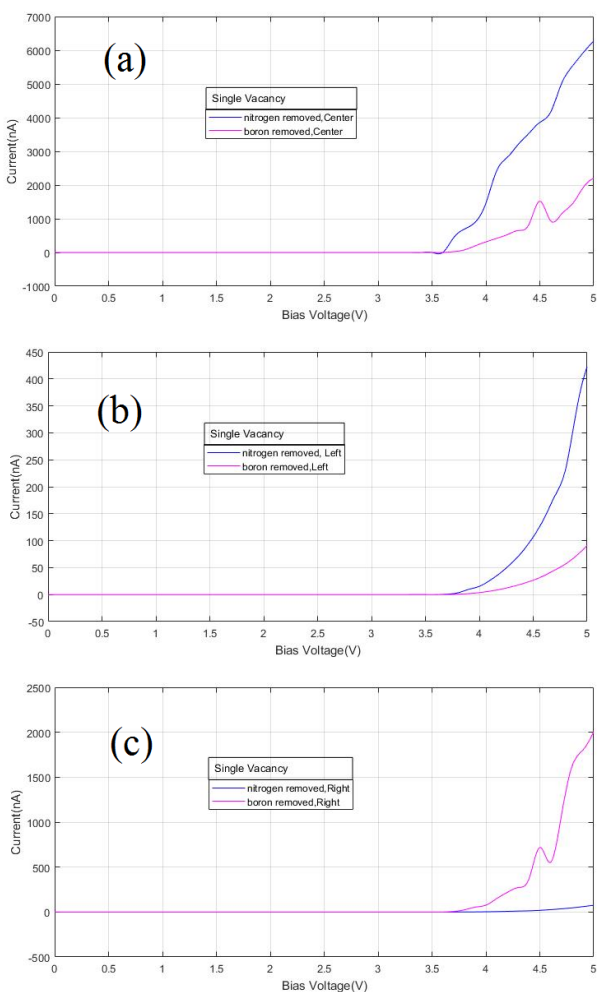
Figure 12. Current-bias voltage curves of the defective BN nanosheet with the nitrogen and boron removed atom (a) center (b) left (c) right.

Figure 13. Conductive characteristics of the pure and defective BN nanosheets with (a) the nitrogen and (b) boron removed atom at different positions.

tric current for the BN nanosheet with nitrogen removed atom.

The effect of defect position on the I–V characteristics of BN nanosheet can also be studied from Fig. 12(a-c). Under the same applied bias conditions, the current depends on the defect position and removed atom type. However, no significant change is observed in the amplitude of the transmission contributing to the current after its initial raise until the bias voltage. Hence one can conclude that the current passing through BN nanosheets is very sensitive to the position of the vacancy defect and removed atoms type.

The decrease and increase in the current flows through the BN nanosheets with different defect positions and removed atoms types at a specific bias voltage can be associated with the variation of their electronic structures, which in turn is caused by the modification of the atomic structure due to the local defect. In mesoscopic physics or molecular electronics, the transmission cannot be obtained directly by using usual transport experiments. Instead of it, the following relation, Landauer Formula, can be used to compute the

zero-bias conductance:

$$G = \frac{dI}{dV}\Big|_{V=0}$$

According to the above equation, the conductance, G, equals the transmission computed at the Fermi energy $G = T(E_f)$ in units of $2e^2/h$, that $G_0 = 2e^2/h$ is quantum conductance. By integrating the $T(E)$ over energy E, the current in the Landauer- equation (Eq. (1)) can be obtained [30, 31].

According to Figs. 13(a-b), the maximum of the conductance peaks of BN nanosheets with single vacancy in center is larger than perfect and other defective nanosheets. By increasing the conductivity, the electric current increases ($G = 1/R$), which can be seen in Figs. 13(a-b).

The calculated phonon transmissions for the semiconductor pure and defective BN nanosheet are shown in figure 14. The phonon transmission variations of defective BN nanosheets are similar but different from the pure structure,
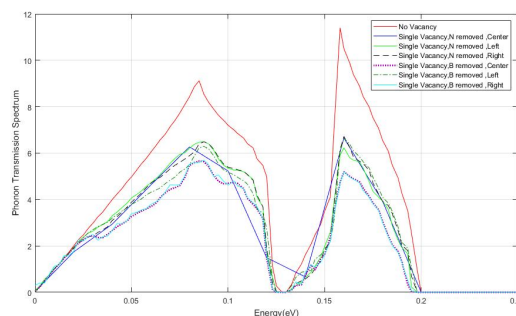
Figure 14. Phonon transmission spectrum energy curves.
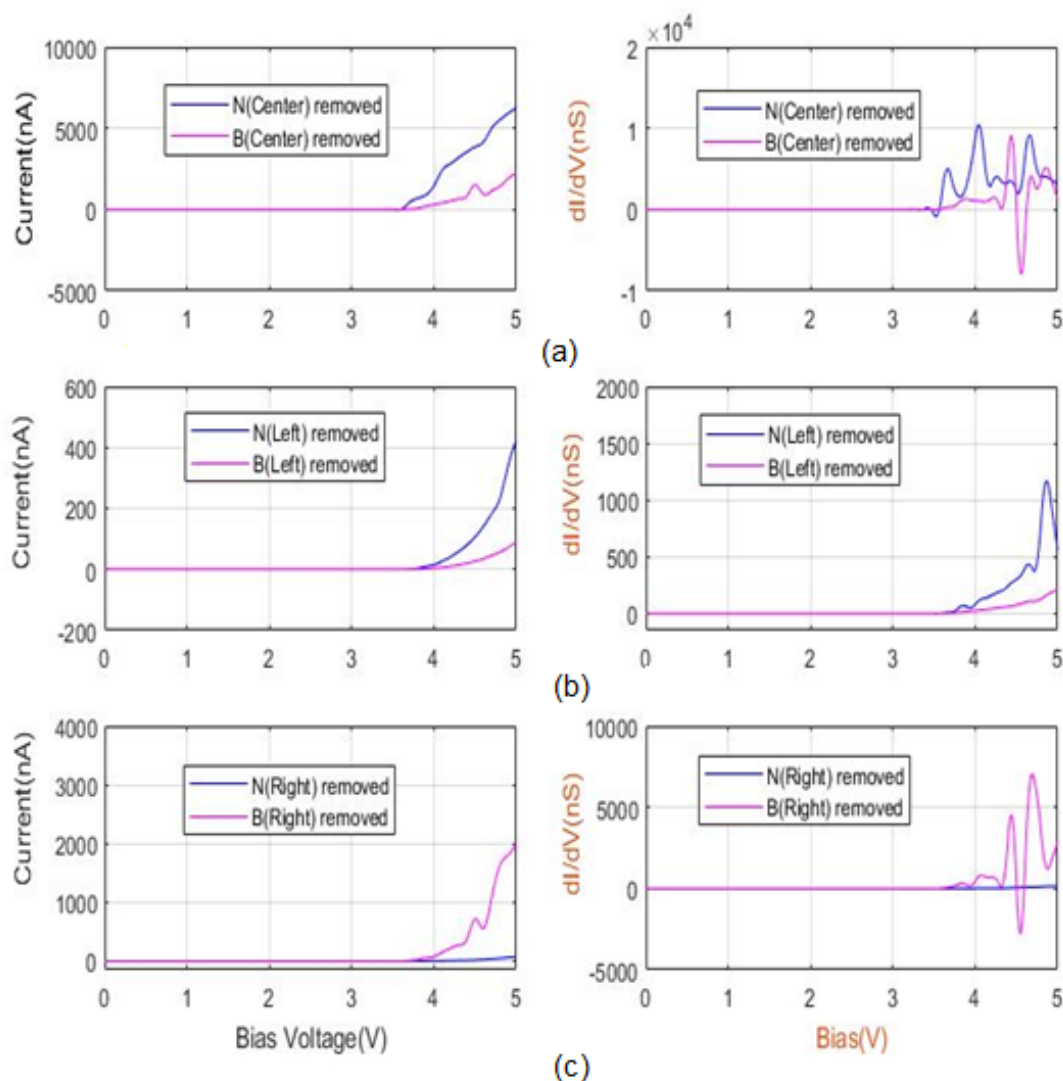
Figure 15. Comparison Current and Conductive Characteristics of the defective nitrogen and boron removed (a) center (b) left (c) right BN nanosheets.

when the size in the transverse direction is confined to 7 unit cells. The total phonon transmissions are divided by the number of unit cells in the cross-section area in order to compare with each other [32–34]. The results for the corresponding bulk system are plotted for comparison. When there is a vacancy defect in the structure, the number of oscillations increases. The oscillations are due to the large number of new phonon modes formed in the structure of defect.

An accurate comparison in Figs 15(a-c) shows that the conductivity of BN nanosheets in which a boron atom is removed from the right side of the nanosheet is greater than that of BN nanosheets in which a nitrogen atom is removed from the right side of the nanosheet which leads to a larger electric current. However, for the atom removed from the left side and center of the nanosheet, the conduction of BN nanosheets with nitrogen removed atom is larger than BN nanosheets with boron removed atom which results in a larger current.

Here, polarization corrections have been ignored. Accord-

ing to this figure, it can be concluded that the peaks of the currents in each diagram match with the conductivity enhancement. Besides, the curves associated with electrical current and conductivity follow a similar pattern. Also, by increasing the applied voltage, the current increases. For case single vacancy located at the center of the nanosheet, increase in the electric current occurs in 3 steps. Here, the steplike behavior indicates opening a new channel.

On the other hand, the transmission-energy curves shown in Figs. 8 represent that the electrical conductivities of the BN nanosheet with centrally removed nitrogen and boron atoms are larger than the nanosheet with the single vacancy defect at the left and right hand sides of the nanosheet. Similarly, comparison of current curves indicates that the electrical currents of the nanosheets with a centrally located single vacancy defect are larger than the nanosheet with the removed atom from the left and right sides, which is confirmed by Eq. (1).

The transmission coefficient is influenced by two parameters, including electronic and the strength of the elec-
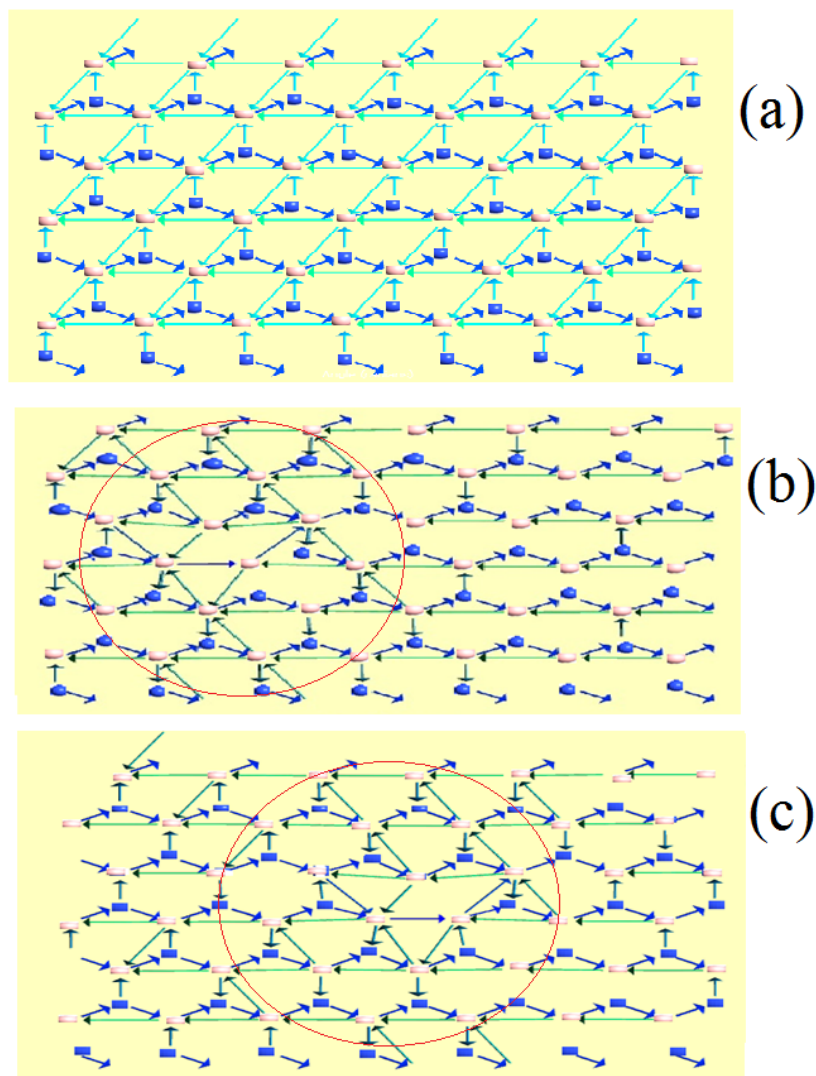
Figure 16. The transmission pathways diagram BN nanosheets (a) without vacancy defect, (b) vacancy defect with nitrogen removed in left and (c) vacancy defect with nitrogen removed in center.Blue squares are nitrogen while pinks are boron.

trode/molecule coupling [35, 36]. Hence, Green's function would be changed by changing the electronic energy of the coupled molecule which results in the change in the density of states (DOS) of the coupled molecule. As it can be seen in the conductivity curves represented in Figs. 15(a-c), the current flow increases by enhancing the amplitude of the picks. This is confirmed by Eq. (1). The difference could be described by the considering tunneling phenomenon through the molecules and besides, the electrical conductors of electrodes.

On the other hand, the conductivity characteristics shown in Figs. 13(a-b) indicate a drop. The largest drop is observed for BN nanosheets with central vacancy defect. In addition, a sharp drop is seen in the conductivity of BN nanosheet with the boron removed atom from the center and right side of the nanosheet. In fact, it can be said that the electric current returns at a certain bias voltage, which corresponds to the electric current curves in Figs 15.

Electronegativity is a chemical property that indicates the tendency of an atom to absorb a pair of common electrons. Due to different electronegativity of boron and nitrogen atoms, unlike the C-C bonds in graphene, the N-B bonds are partially polar. Electronegativity is mostly used to describe the polarity of a bond. In general, the greater the electronegativity differences between two bonded atoms, the greater the polarity of the bond. In two bonded atoms, an atom with larger electronegativity would be the negative end of the bond.

The polarity of the structure of BN nanosheets in which the atom has been removed from the center of the nanosheet is larger than other structures. Besides, the polarity of the structure of BN nanosheets in which a nitrogen atom has been removed from the center of the nanosheet is larger than that of boron removed atom. In a nanosheet in which a boron atom has been removed, there are more nitrogen atoms than boron atoms. While, in a nanosheet in which a nitrogen atom has been removed, the number of boron atoms would be larger than nitrogen atoms. Since the electronegativity of nitrogen is larger than that of boron, the current return in the latter structure is larger and the conductivity is smaller. To further investigate the negative conductivity, the transmission pathways diagram is plotted in Figs. 16(a-c)

for some arbitrary states.

Figures 16 show the transmission pathways diagram of BN nanosheets for some arbitrary state. According to this figure, the transmission pathways in the BN nanosheets without defect are perfectly regular. Comparison of the transmission pathways of the pure BN nanosheet and the nanosheets with the defect on the left and the center shows that the pure nanosheets possess smaller density of transmission pathways lines. It can be said that the number of pure lines of the output path is larger for pure nanosheets. This indicates a larger transfer and consequently a larger current flux. In other words, at a certain energy and voltage, the density and irregularity of transmission lines in the area of defect (red circle) are greater and as a result, the net transmission lines are in the original opposite directions, which indicates the return current and also reduction in conductivity.

4. Conclusion

In this paper, the transport properties of a perfect and defective BN nanosheet with single vacancy defect were studied and the effect of vacancy defect on the structure and electronic properties of the BN nanosheets were evaluated. It was shown that in addition to the defect, the type of removed atom and the position of the vacancy defect have a considerable influence on the transport spectra and I–V characteristics of the BN nanosheets. Especially, the current under a constant bias can be altered by applying local vacancy defect. The trend of the current variation by applying the vacancy depends on the vacancy position, removed atom type of removed and changing in the electronic structures of BN nanosheets. Also, this study shows the electronic band structure and total density of states (DOS) corresponding to the boron nitride nanosheet. The result shows that the peak height of the N removed in center of BN nanosheets increases greatly and the electron conduction increases because the availability of the state around Fermi energy increases.

In addition to the I-V curve, the transmission and conductance characteristics of the BN nanosheets also depend on the defect position and type of the removed atom which indicates the high sensitivity of electronic transmission characteristics to the location of the vacancy. The results also show that as the voltage increases, the electrical conductivity changes. At voltages larger than 3 V, electrical conductivity of a BN nanosheet with centrally located single vacancy defect would be larger than other considered cases. On the other hand, with these applied conditions, negative conductivity was observed which can be interpreted by changing the structure and the density of transmission pathways.

Conflict of interest statement
The authors declare that they have no conflict of interest.

References

[1] P. T. Mathew and F. Fang. *Engineering*, **4**:760, 2018.

[2] M. Yaghobi and M. R. Niazian. *Brazilian Journal of Physics*, **44**:687, 2014.

[3] S. Iijima. *Nature*, **354**:56, 1991.

[4] M. B. Nardelli. *Phys. Rev. B*, **60**:7828, 1999.

[5] L. Zhou and J. P. Carbotte. *Phys. Rev. B*, **421**:97, 2013.

[6] N. A. Zimbovskaya and M. M. Kuklja. *The Journal of Chemical Physics*, **131**:114703, 2009.

[7] S. S. Siwal, A. K. Saini, S. Rarotra, Q. Zhang, and V. K. Thakur. *Journal of Nanostructure in Chemistry*, **11**:93, 2021.

[8] D. Golberg, Y. Bando, Y. Huang, T. Terao, M. Mitome, C. Tang, and C. Zhi. *ACS Nano.*, **4**:2979, 2010.

[9] M. R. E. Tanjil, Y. Jeong, Z. Yin, W. Panaccione, and M. C. Wang. *Coatings*, **9**:133, 2019.

[10] X. Wang, C. Zhi, Q. Weng, Y. Bando, and D. Golberg. *J. Phys.: Conf. Ser.*, **471**:0102003, 2013.

[11] M. Brandbyge, J. L. Mozos, P. Ordej´ón, J. Taylor, and K. Stokbro. *Physical Review B*, **65**:165401, 2002.

[12] M. Brandbyge, K. Stokbro, J. Taylor, J. L. Mozos, and P. Ordej´ón. *Physical Review B*, **67**:193104, 2003.

[13] J. Zhang, R. Sun, D. Ruan, M. Zhang, Y. Li, K. Zhang, F. Cheng, Z. Wang, and Z. Wang. *Journal of Applied Physics*, **128**:100902, 2020.

[14] P. Sutter, R. Cortes, J. Lahiri, and E. Sutterm. *Nano Lett.*, **12**:4869, 2012.

[15] S. Smidstrup, T. Markussen, P. Vancraeyveld, J. Wellendorff, J. Schneider, T. Gunst, B. Verstichel, D. Stradi, P. A. Khomyakov, and et al. *Journal of Physics: Condensed Matter*, **32**:015901, 2019.

[16] F. Oliveira, G. Seifert, T. Heine, and H. A. Duarte. *J.Braz.Chem.Soc*, **20**:7, 2009.

[17] D. Porezag, T. h. Frauenheim, T. h. K¨öhler, G. Seifert, and R. Kaschner. *Phys. Rev. B*, **51**:12947, 1995.

[18] G. Seifert, D. Porezag, and T. Frauenheim. *Int. J. Quantum Chemistry*, **58**:185, 1996.

[19] P. W. Fowler, D. Mitchell, D. Porezag, and T. Frauenheim. *Chemical Physics Letters*, **268**:352, 1997.

[20] A. Pecchia and A. Di Carlo. *Rep. Prog. Phys.*, **67**:1497, 2004.

[21] A. Pecchia, A. Di Carlo, A. Gagliardi, S. Sanna, Th. Fraunheim, and R. Gutierrez. *Nano Lett.*, **4**:2109, 2004.

[22] A. D. Carlo, M. Gheorghe, P. Lugli, M. Stenberg, G. Seifert, and Th. Frauenheim. *Physica B*, **314**:86, 2002.

[23] J. Taylor, H. Guo, and J. Wang. *Physical Review B*, **63**:24, 2001.

[24] M. R. Niazian and M. Yaghobi. *IJPAP*, **54**:123, 2016.

[25] J. Wang, F. Ma, W. Liang, and M .Sun. *Materials Today Physics*, **2**:6, 2017.

[26] J. Yin, J. Li, Y. Hang, J. Yu, G. Tai, X. Li, Z. Zhang, and W. Guo. *Small*, **12**:22, 2016.

[27] J. Jia, D. Shi, X. Feng, and G. Chen. *carbon*, **76**:54, 2014.

[28] P. Sutter, R. Cortes, J. Lahiri, and E. Sutterm. *Nano Lett.*, **12**:4869, 2012.

[29] M. R. Niazian, L. F. Matin, M. Yaghobi, and A. A. Masoudi. *Current Nanoscience*, **16**:936, 2021.

[30] P. Zhang. *nature*, **5**:9826, 2015.

[31] S. Lu and A. J. H. Mc Gaughey. *Journal of Applied Physics*, **121**:115103, 2017.

[32] Y. Xue, Q. Liua, G. He, K. Xu, L. Jiang, X. Hu, and J. Hu. *Nanoscale research letters*, **8**:49, 2013.

[33] T. Li, C. He, and W.Zhang. *Journal of Energy Chemistry*, **52**:121, 2021.

[34] W. X. Zhang, Y. Yin, and C. He. *Journal of Physical Chemistry Letters*, **12**:5064, 2021.

[35] R. Beiranvand and S. Valedbagi. *Diamond and Related Materials*, **58**:190, 2015.

[36] B. Hu, H. Guo, Q. Wang, W. Zhang, S. Song, X. Li, Y. Li, and B. Li. *Composites Part A: Applied Science and Manufacturing*, **137**:106038, 2020.